A Study of the Assembly Mechanism of the Mesoporous MSU-X Silica Two-Step Synthesis

Cedric Boissière,[†] André Larbot,[†] Claudie Bourgaux,[‡] Eric Prouzet,*[,†] and Clifford A. Bunton[§]

Laboratoire des Matériaux et Procédés Membranaires (IEM) (CNRS UMR 5635), CNRS, 1919 Route de Mende, F-34293 Montpellier Cedex 5, France, Laboratoire pour l'Utilisation du Rayonnement Synchrotron (CNRS UMR 5635), Bat 209D, Centre Universitaire Paris Sud, BP 34, F-91898 Orsay Cedex, France, and Department of Chemistry and Biochemistry, University of California at Santa Barbara, Santa Barbara, California 93106

Received February 5, 2001

Several synthetic pathways of mesostructured porous silica using nonionic surfactants or copolymers have been reported since the discovery of this new family of materials. We developed a process, which we call a two-step synthesis, that allows us to synthesize MSU-X mesoporous silica, with very good reproducibility and high reaction yields. This reaction implies a first assembly step between silica oligomers and nonionic micelles, followed by a condensation step induced by the addition of sodium fluoride as catalyst. We characterized nanoscopic hybrid objects made of silica and nonionic poly(ethylene oxide) (PEO) surfactants obtained once the assembly between silica and surfactants had occurred, as intermediates in the two-step synthesis of mesoporous silica of the MSU-X family. NMR, small-angle X-ray scattering, and dynamic light scattering experiments allowed us to propose a structural model involving nucleophilic participation of external OH groups, where a low-density framework of silica grows out of the micellar hydrophilic outer shell made of PEO chains, and builds a third shell around the initial spherical micelle. Stable and isolated micellar hybrid objects with this three-layered structure (alkyl core, PEO first shell, silica second shell) were observed, forming monodisperse objects with diameters adjustable between 7 and 12 nm, depending on the amount of silica.

I. Introduction

Mesoporous micelle-templated structures (MTSs) first reported by a Mobil group,[1] and then by Inagaki et al.,[2] are usually obtained through an assembly mechanism where organic species, ionic or nonionic surfactants, or copolymers interact with inorganic precursors of the future inorganic framework. These reactions form highly structured materials, exhibiting hexagonal (MCM-41, SBA-15) or cubic (MCM-48, SBA-1) symmetries of the porous framework, or a 3D wormhole porosity (e.g., HMS, MSU-X).[3] For cationic surfactants, e.g., of quaternary ammonium ions, charge balance with electrostatic interactions among surfactants, inorganic ions, and/or counterions plays a major role.[4] EPR in situ investigations by Galarneau et al. reported that MCM-41 assembles through a rapid initial step where surfactants and silicates form an amorphous gel.[5] The hexagonal structure is then built within this gel by local reorganization similar to that for a zeolite A.[6] This conclusion differs from the initial suggestion that hybrid rodlike micelles surrounded by aluminosilica layers may associate to give growing hexagonal stacking.[1,7] However, accurate studies are difficult because all the syntheses developed since the discovery of these new materials involve overlapping of the assembly step between surfactants and inorganic precursors and the condensation step of the inorganic species generating the inorganic skeleton. Hence, it is difficult to identify the precursors of such mesoporous materials.

Since 1994, several syntheses employing poly(ethylene oxide) (PEO) nonionic surfactants or copolymers have been reported.[8−12] Since the first report of an actual assembly mechanism involving these classes of surfactants,[8] various porous structures have been re-

* To whom correspondence should be addressed. E-mail: prouzet@iemm.univ-montp2.fr.
[†] CNRS.
[‡] Centre Universitaire Paris Sud.
[§] University of California at Santa Barbara.

(1) Kresge, C. T.; Leonowicz, M. E.; Roth, W. J.; Vartuli, J. C.; Beck, J. S. *Nature* **1992**, *359*, 710.
(2) Inagaki, S.; Fukushima, Y.; Kuroda, K. In *Zeolites and Related Microporous Materials: State of the Art*; Weitkamp, J., Karge, H. G., Pfeifer, H., Hölderich, W., Eds.; Elsevier Science: New York, 1994; Vol. 84, p 125.
(3) Beck, J. S.; Vartuli, J. C. *Curr. Opin. Solid State Mater. Sci.* **1996**, *1*, 76.
(4) Huo, Q.; et al. *Nature* **1994**, *368*, 317.
(5) Galarneau, A.; Di Renzo, F.; Fajula, F.; Mollo, L.; Fubini, B.; Ottaviani, M. F. *J. Colloid Interface Sci.* **1998**, *201*, 105.
(6) Mintonva, S.; Olson, N. H.; Valtchev, V.; Bein, T. *Science* **1999**, *283*, 958.
(7) Beck, J. S.; et al. *J. Am. Chem. Soc.* **1992**, *114*, 10834.
(8) Bagshaw, S. A.; Prouzet, E.; Pinnavaia, T. J. *Science* **1995**, *269*, 1242.
(9) Attard, G. S.; Glyde, J. C.; Göltner, C. G. *Nature* **1995**, *378*, 366.
(10) Zhao, D.; Feng, J.; Huo, Q.; Melosh, N.; Fredrickson, G. H.; Chmelka, B. F.; Stucky, G. D. *Science* **1998**, *279*, 548.
(11) Prouzet, E.; Pinnavaia, T. J. *Angew. Chem., Int. Ed. Engl.* **1997**, *36*, 516.
(12) Voegtlin, A. C.; Ruch, F.; Guth, J. L.; Patarin, J.; Huve, L. *Microporous Mater.* **1997**, *9*, 97.

10.1021/cm011031b CCC: $20.00
Published on Web 09/18/2001

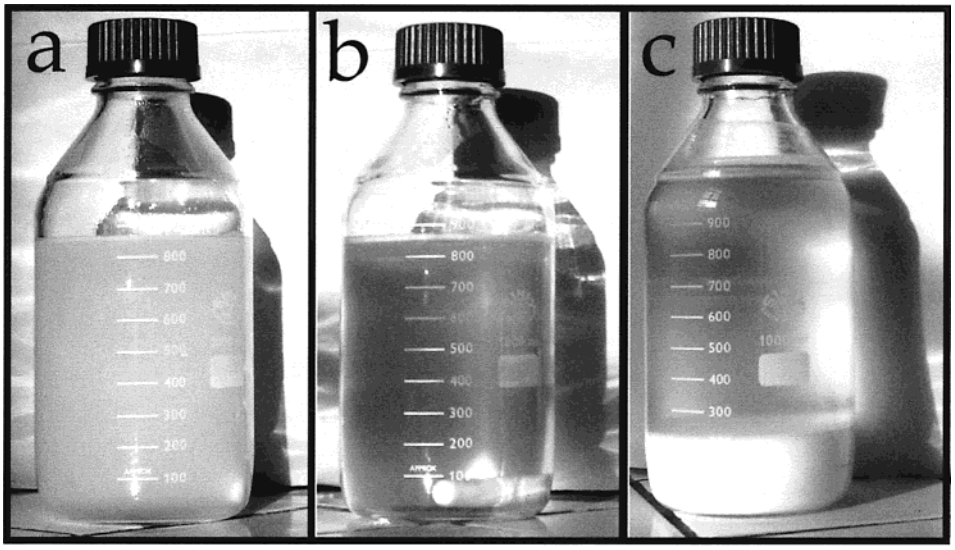

Figure 1. Graphs of the reacting medium (a) after addition of TEOS (Si/surfactant molar ratio 8) in a 0.02 mol·L^{-1} solution of Tergitol 15S12 ($C_{15}(EO)_{12}$) at pH 6, (b) after adjustment to pH 2, and (c) 3 days after the addition of NaF (F/Si = 2 mol %).

ported ranging from 3D wormhole (MSU-X materials)[8] to hexagonal.[10,13,14] We reported recently that MSU-X silica could be synthesized in a controlled process, which is a fluoride-assisted two-step synthesis pathway, where the assembly step of silica precursors with micelles can be clearly separated from silica condensation. In a first step, hydrolysis of a silicon alkoxide in a nonionic surfactant solution, in a pH range where no condensation occurs, gives within minutes a stable solution where hybrid objects made of nonionic micelles and silica oligomers are expected to form. The silica condensation is further assisted in a second step by a catalyst such as sodium fluoride.[15−17] To improve our understanding of that process, we carried out specific analyses to get more detailed information on the structure of the objects expected to exist after the silica hydrolysis reaction, in mild acidity with the presence of nonionic PEO surfactants, and to confirm that our first reaction step is the actual assembly step. We therefore undertook specific characterizations by using several techniques including liquid ^{29}Si NMR, small-angle X-ray scattering (SAXS), and dynamic light scattering (DLS). We report herein a model that describes the formation of organic−inorganic micellar entities built through a specific assembly mechanism allowed only by the two-step synthesis of MSU-X silica, which we reported previously.[15]

II. Experimental Section

II.1. Synthesis. The synthesis first proceeds from addition under mechanical stirring of a silica alkoxide (TEOS, $Si(OCH_2CH_3)_4$) (ACROS) to a 0.02 M solution of a nonionic surfactant such as Tergitol 15-S-12 ($CH_3(CH_2)_{14}(EO)_{12}$) (kindly provided by Union Carbide Co.). In a current synthesis, the usual Si/surfactant molar ratio is 8 ([TEOS] = 0.16 mol·L^{-1}), but reactions have been performed with Si/surfactant ratios from 4 to 12. TEOS being insoluble in water and not reacting under neutral pH, one obtains a cloudy emulsion (see Figure 1a). At this point, the acidity is adjusted in a 2−4 pH range by the addition of 0.2 M hydrochloric acid (this addition can also be performed before the TEOS addition). It should be noted that acidification does not induce the silica condensation as reported in other work.[10,18,19] Within minutes, the initial emulsion clarifies (Figure 1b) and a solution, stable for days, is obtained, whose formation is the purpose of our present report. Finally, after addition of a small amount of fluoride ion (F^-/Si = 1−6 mol %), a well-known silica condensation catalyst,[20] a powder settles at the bottom of the container (Figure 1c). After filtration, drying, and calcination in air (6 h, 620 °C), micrometric spherical particles are obtained, which exhibit the expected features of MSU-X materials, that is, a single X-ray diffraction (XRD) peak characteristic of the wormhole porous framework, and a narrow pore size distribution without any textural porosity.[15,16]

II.2. Experimental Procedures. DLS analyses were performed at 20.1 °C, on a Brookhaven BI-9000AT computing autocorrelator. Scattered light from an Optila argon ion (λ = 480 nm) laser was collected from one coherence area at 90° and imaged onto the 100 μm slit of an Amamasu HC120 photomultiplier. All DLS curves fit a single-exponential function, showing that light scatterers remain largely monodisperse. Micellar diameters were deduced from the diffusion coefficient by using the Stokes−Einstein relationship. SAXS experiments were conducted at the D24 beamline of the Lure-DCI synchrotron radiation source (France, Orsay). The single-crystal curved monochromator provided a beam focused in the horizontal plane. The selected wavelength was 1.49 Å. The beam size (typically 0.4 × 1.5 mm^2) was determined by collimation slits downstream from the monochromator. To reduce absorption and parasitic scattering, the beam path was kept under vacuum and antiparasitic slits were placed before the sample. An ionization chamber monitored the beam intensity. The sample-to-detector distance was adjusted to cover the required scattering vector range. The scattering patterns were recorded with a gas-filled, position-sensitive detector. For the in situ study of pure TEOS gelation, spectra

(13) Zhao, D.; Huo, Q.; Feng, J.; Chmelka, B. F.; Stucky, G. D. *J. Am. Chem. Soc.* **1998**, *120*, 6024.
(14) Bagshaw, S. A. In *Mesoporous Molecular Sieves 1998*; Bonneviot, L., Beland, F., Danumah, C., Giasson, S., Kaliaguine, S., Eds.; Elsevier Science: Amsterdam, 1998; Vol. 117, p 381.
(15) Boissière, C.; van der Lee, A.; El Mansouri, A.; Larbot, A.; Prouzet, E. *J. Chem. Soc., Chem. Commun.* **1999**, *20*, 2047.
(16) Boissière, C.; Larbot, A.; van der Lee, A.; Kooyman, P. J.; Prouzet, E. *Chem. Mater.* **2000**, *12*, 2902.
(17) Boissière, C.; Larbot, A.; Prouzet, E. *Chem. Mater.* **2000**, *12*, 1937.
(18) Brinker, C. J. *J. Non-Cryst. Solids* **1988**, *100*, 31.
(19) Schmidt-Winkel, P.; Yang, P.; Margolese, D. I.; Chmelka, B. F.; Stucky, G. D. *Adv. Mater.* **1999**, *11*, 303.
(20) Corriu, R. J. P.; Leclercq, D.; Vious, A.; Pauthe, M.; Phalippou, J. In *Ultrastructure Processing of Advanced Ceramics*; Mackenzie, J. D., Ultrich, D. R., Eds.; Wiley: New York, 1988; Vol. 113.

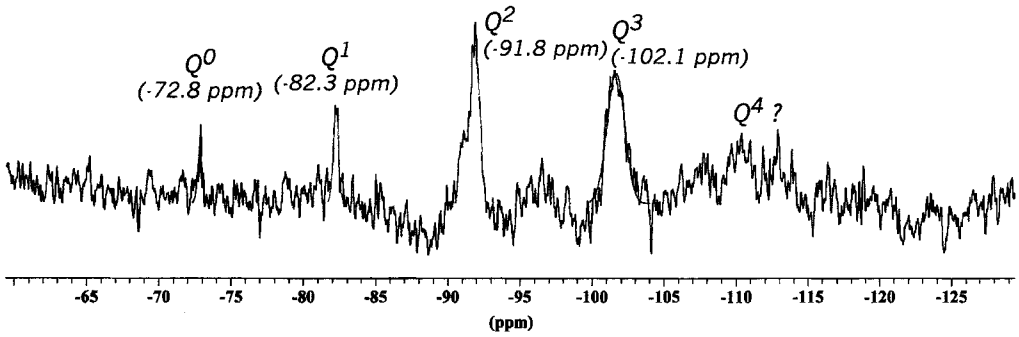

Figure 2. ^{29}Si NMR spectrum of a 0.24 mol·L^{-1} aqueous solution of TEOS hydrolyzed at pH 2.

were recorded for 3 min every 15 min. Micellar solution spectra were recorded three times over 10 min and were averaged. The in situ study of the reaction itself was performed by 3 min long successive recordings started at addition of the fluoride salt. ^{29}Si{^{1}H} NMR measurements were performed on a Bruker AC 250 spectrometer operating at 49.69 MHz. The sample solution was placed into a 10 mm glass NMR tube which was rotated at 15 Hz. The spectrum was recorded with external lock (DMSO-d_6) and obtained with gated decoupling and repetition times of 30 s. The spectrum width was 5000 kHz, and 32K data points were used. The chemical shifts are referred to tetramethylsilane. The quantitative analysis of line intensities was carried out off line with WIN-NMR software. Depending on the signal-to-noise ratio, error margins of the integration were estimated to be ±10%. Classical Q notation was used for the different silicate species depending on the number of oxygen bridging atoms: *i* represents the number of oxo bridges. The term Q^i is used for tetrameric species which have *i* siloxane (Si−O−Si) bonds. The literature provides information on the average chemical shift ranges of Q^0, Q^1, Q^2, Q^3, and Q^4 species.[21−23]

III. Results

III.1. Hydrolysis and Condensation of Aqueous Solutions of TEOS without Surfactant. Unlike the usual alkoxide-based sol−gel processes, our reaction involves an aqueous instead of an alcoholic medium. Therefore, we studied first the structure of silica oligomers built by the hydrolysis of TEOS (0.24 mol·L^{-1}), in a pure aqueous medium acidified at pH 2. At this acidity, close to the isoelectric point of silica, the hydrolysis is fast and the extent of condensation is low.[18] SAXS does not detect any scattering object, which implies that the solution does not contain colloidal particles but small silica oligomers. ^{29}Si liquid NMR (Figure 2) shows that Q^0, Q^1, Q^2, and Q^3 can be clearly identified, but the existence of Q^4 remains questionable. Despite the low signal-to-noise ratio, one can estimate a rough Q^2/Q^3 ratio of about 50/50. Hence, it appears that the main part of the silica that results from the hydrolysis of TEOS at pH 2 is made of small unconnected oligomers.

The polymerization of these silica oligomers was induced by the addition of sodium fluoride with a 2 mol % F/Si ratio. The reaction was followed by in situ SAXS measurements on 0.08, 0.24, and 0.4 mol·L^{-1} initial TEOS aqueous solutions, hydrolyzed at pH 2. Unlike the MSU-X synthesis implying an assembly between silica and surfactants, which gives a powder, a gel is obtained when pure TEOS is hydrolyzed alone. Changes in intensities for the first moments of reaction are displayed in Figure 3. Although, different kinetic trends are observed, depending on the concentration, the global tendencies are similar, whatever the initial concentration. The medium evolves toward a monolithic gel that exhibits a similar scattering pattern with the same Porod slope over the whole recorded wave vector range. After 30 h, this slope is −1.88, and the SAXS patterns are only slightly modified upon aging since the Porod slope reaches the value −2.0 after 30 days. Surprisingly,

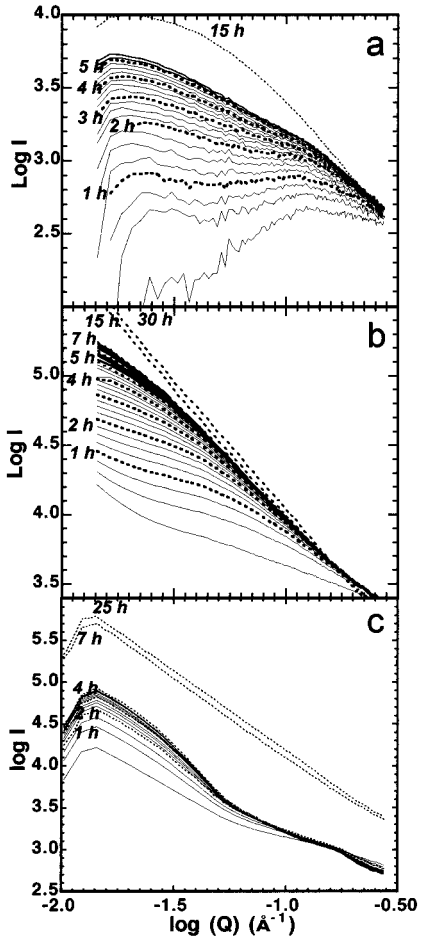

Figure 3. Evolution with time of the X-ray small-angle scattering of gelifying aqueous solutions starting from silica oligomers obtained by hydrolysis of TEOS in an acid aqueous solution (pH 2), with different silica concentrations: (a) 0.08 mol·L^{-1}, (b) 0.24 mol·L^{-1}, and (c) 0.4 mol·L^{-1}. Time zero refers to the addition of sodium fluoride (F/Si = 2 mol %).

(21) Kelts, L. W.; Effinger, N. J.; Melpolder, S. M. *J. Non-Cryst. Solids* **1986**, *83*, 353.
(22) Pouxviel, J. C.; Boilot, J.-P.; Beloeil, J. C.; Lallemand, J. Y. *J. Non-Cryst. Solids* **1987**, *89*, 345.
(23) Assink, R. A.; Kay, B. D. *Annu. Rev. Mater. Sci.* **1991**, *21*, 491.

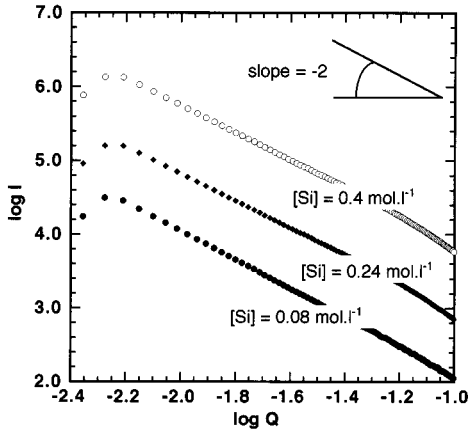

Figure 4. X-ray small-angle scattering of the silica gels after a 30 day aging. Curves were vertically shifted to aid clarity.

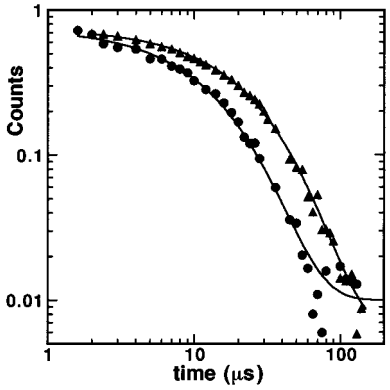

Figure 5. Correlation function calculated from the dynamic light scattering of a solution of nonionic micelles of Tergitol 15S12 (0.02 mol·L^{-1}) (circles) acidified to pH 2 and a mixture of TEOS and surfactant with a Si/surfactant molar ratio of 23 (triangles). Lines correspond to the monoexponential fit performed on each curve.

the initial TEOS concentration does not affect the structure of the aged gels (Figure 4). They exhibit the same fractal structure, with a Porod slope that corresponds to a low reticulated silica framework.[18]

III.2. Hydrolysis and Condensation of Aqueous Solutions of TEOS with Surfactant. At the intermediary step of the reaction (Figure 1b), the aqueous solution is expected to contain micellar objects, but the question is whether silica oligomers interact with the nonionic micelles at this stage. Nevertheless, TEOS can be added to the 0.02 mol·L^{-1} surfactant solution at pH 2−4, up to a final Si/surfactant mole ratio of 23, without organic-rich and aqueous-rich phase separation or silica precipitation. Two representative correlation functions calculated from DLS are displayed in Figure 5, along with their exponential fits. The obvious difference between the correlation functions of the Si/surfactant = 0 and the Si/surfactant = 23 samples proves that there is an actual interaction between silica oligomers and the micelles, which modifies the micellar size. All scattering was fitted with good agreement by using a single-exponential fit, that is, assuming monodisperse objects. Figure 6 displays the evolution of the diameters as a function of the molar Si/surfactant ratio. Pure Tergitol 15S12 micelles have a mean hydrodynamic diameter of 6.8 nm, which remains constant up to a Si/surfactant mole ratio of 4. For higher ratios, one

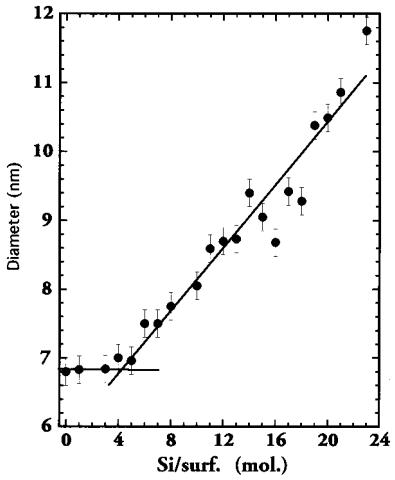

Figure 6. Evolution of the apparent hydrodynamic diameter from DLS of the micellar hybrid objects as a function of the Si/surfactant mole ratios.

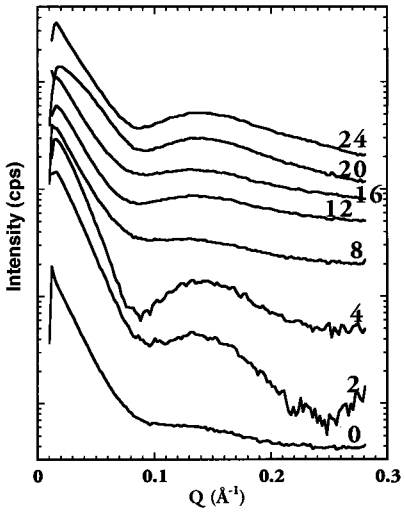

Figure 7. Evolution of the X-ray small-angle scattering of solutions prepared with different Si/surfactant molar ratios (see the right side of the curve).

observes a linear size increase up to ca. 12 nm. Compared with the drastic changes observed with DLS, SAXS patterns of these solutions exhibit only slight modifications (Figure 7). There are minima at ca. Q = 0.9 Å^{-1} that can be assigned to a characteristic length varying from ca. 6.6 to 7.3 nm for Si/surfactant = 0 and 4, respectively This distance is consistent with the Tergitol micellar diameter. The positions of these minima, that is, sizes probed by SAXS, remain constant and equal to 0.085 Å^{-1} for higher ratios. The main change regards the intensity of the peak observed between 0.1 and 0.2 Å^{-1}. Its intensity increases strongly for Si/surfactant ratios of 2 and 4 and then decreases and becomes rather constant for higher ratios.

Once the fluoride ion has been added (F/Si ratio 4 mol %), the initial step of the polymerization reaction at room temperature was followed by SAXS, with continuous in situ recordings (each over 3 min) (Figure 8). There is a fast change in the system, and within 10 min (dashed pattern), the correlation peak, the fingerprint of the mesostructured network, begins to grow at Q = 0.12 Å^{-1}, whereas the broad peak observed with unperturbed micellar solutions still remains.

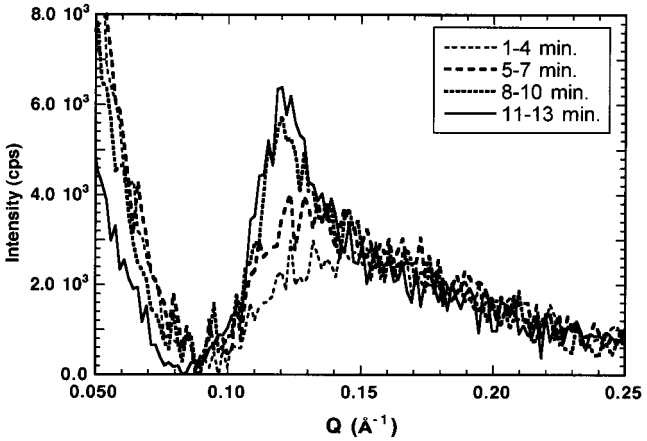

Figure 8. Evolution of the X-ray small-angle scattering of a solution prepared with a Si/surfactant molar ratio of 8, after the addition of sodium fluoride (time 0). The key corresponds to the time recording range after the addition of NaF.

IV. Discussion

In the pH 2−4 range, the TEOS hydrolysis is fast whereas silica condensation is slow.[16,18] Therefore, TEOS can be quickly hydrolyzed in water at pH 2−4, but it gives stable small oligomers (SAXS does not detect any scatterer) that are little reticulated (our ^{29}Si NMR spectra, displayed in Figure 2, of solutions of pure silica hydrolyzed at pH 2 reveal mainly Q^2 and Q^3 signals). The tendency of these oligomers, when one adds a polymerization catalyst, such as sodium fluoride, is to build a low-density gel. These oligomers polymerize in an open network characterized by a low fractal dimension (Porod slope ∼−2) instead of a dense silica framework (Porod slope then expected to be −3) (see Figures 3 and 4). Surprisingly, the gel structure does not depend on the initial TEOS concentration (between 0.08 and 0.4 mol·L^{-1}). This result, which we did not explore further, seems to arise from the connection mode adopted for the silica oligomers.

On the other hand, the general behavior of the hydrolysis and condensation of TEOS, in the presence of nonionic surfactants, is totally different, as can be easily checked by the MSU-X reaction itself: with surfactants, one obtains a powder of spherical micrometric particles instead of a monolithic gel. When TEOS is added to the surfactant solution, at pH 2−4, our results show clearly that the interaction between silica oligomers and surfactant micelles occurs at this step, as expected. Dynamic light scattering identifies monodisperse objects whose size changes with increasing amount of TEOS (Figure 5). We added up to a Si/surfactant molar ratio of 23 and still obtained isolated monodisperse objects, without any phase demixing, reaction, or aggregation. Below the Si/surfactant molar ratio of 4, DLS does not detect any obvious size change, but above this value, the diameter increases linearly with the addition of the alkoxide up to a value of 12 nm (Figure 6). Though it is clear that silica interacts with the micelles at this stage of the reaction, one cannot link this interaction with only a swelling effect in the hydrophobic core because such swelling alone could not accommodate such an amount of TEOS or silica oligomers.

The SAXS scattering curves reported in Figure 7 have been identified as characteristic of PEO-based nonionic micelles.[24] The minima correspond to a correlation length characteristic of the micellar diameter, and the second maximum at 0.15 Å^{-1} is assigned to the hydrophilic PEO outer shell. There are no obvious changes, except the shift of the minima from 0.09 to 0.08 Å^{-1}, for Si/surfactant varying from 0 to 4, which corresponds to a size increase from 6.8 to 7.3 nm—this variation being too small to be reliably detected by DLS. The main feature of these patterns is the scattered intensity variation observed for the samples with Si/surfactant = 2 and 4.

To explain the apparent contradiction between DLS and SAXS results, it must be noted that DLS probes moving objects (apparent hydrodynamic radii are deduced from diffusion coefficients through the Stokes−Einstein relation) whereas SAXS probes electron density contrast. Bearing this difference in mind, one can thus propose a growth model for these micellar objects. Interactions of EO groups with silica surfaces have long been reported.[25] Hence, silicate oligomers from TEOS hydrolysis are expected to interact with PEO chains rather than remain in solution or go into the alkyl core. For Si/surfactant = 0−4, DLS results indicate that these silicate oligomers from TEOS hydrolysis enter the micellar palisade layer because the overal diameter does not change. Correspondingly, SAXS detects little change in the micellar size for this Si/surfactant mole ratio range, which proves that silicates do not swell the micellar hydrophobic core but go into the hydrophilic palisade layer of flexible PEO chains. The small 6.8−7.3 nm diameter increase can thus be explained by a slight elongation of the PEO chains. El Moujahid et al. performed small-angle neutron scattering on this type of nonionic micelles.[24] They demonstrated that the shape and intensity of the second maximum, at 0.15 Å^{-1}, is highly dependent on the whole composition of the hydrophilic shell. Unlike SANS, SAXS is sensitive to the electron density contrast, but similar conclusions can be drawn. If silica oligomers go into the PEO palisade layer, the outer shell (PEO + silica) electron density increases, relative to the surrounding water, which explains the intensity increases observed for the Si/surfactant = 2 and 4 mole ratios in this region of the SAXS pattern. Hence, the first stages of the assembly process can be described as the insertion of silica oligomers into the PEO hydrophilic shell, which induces a small lengthening of the chains.

From Si/surfactant = 5 to Si/surfactant = 24, DLS shows that the diameters increase linearly up to almost 12 nm, with a monodisperse size distribution (Figures 5 and 6). Unlike the accepted scheme of formation of the MCM-41-type materials,[7] this size increase cannot be due to the formation of a dense silica wall around the micelle, because the diameter should vary as the cube root of the Si/surfactant ratio. SAXS studies show that F^--catalyzed condensation of silica in aqueous solution (i.e., without surfactant) in this range of concentration and pH evolves toward low-density gels

(24) El. Moujahid, C.; Ravey, J. C.; Schmitt, V.; Stébé, M. J. *Colloids Surf., A* **1998**, *136*, 289.
(25) Tiberg, F.; Brinck, J.; Grant, L. M. *Curr. Opin. Colloid Interface Sci.* **2000**, *4*, 411.

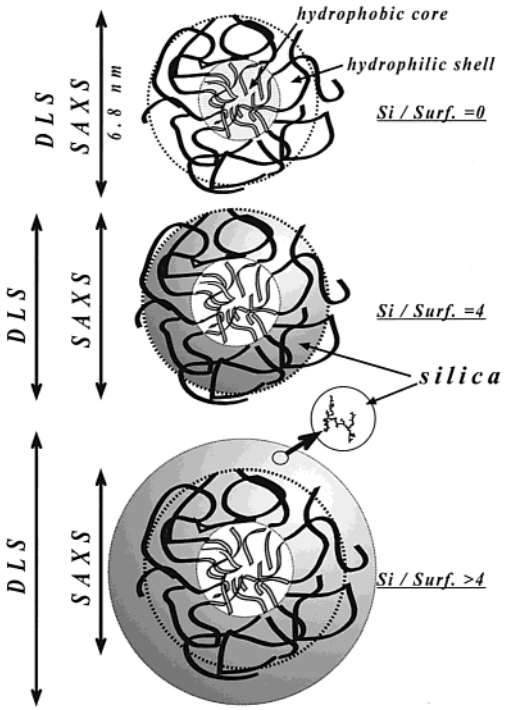

Figure 9. Schematic drawing of the shape and evolution of the hybrid micellar objects, as probed by DLS and SAXS. Vertical arrows indicate the dimensions probed by each of the techniques.

(fractal dimension of 2) (Figures 3 and 4). Such a low density is observed with weakly reticulated gels.[18] Both the weak connections of the initial silica oligomers (Figure 2) and the growth mechanism of pure silica gels in this pH range (Figure 3) indicate that the linear size increase, with the Si/surfactant ratio shown by DLS (Figure 6), demonstrates radial growth ouside the palisade layer of a low-reticulated silica shell, starting from the PEO shell and growing into the medium. This silica shell is not detected by SAXS because it is too dilute to induce significant electron density variations, compared with the electron density of the neighboring water (in-shell calculated $[H_2O]/[Si] = 31/1$; see the Appendix). However, the electron density contrast between the PEO shell (PEO + silica) and the adjacent region (water + silica) decreases, giving the intensity decrease observed in the SAXS patterns for Si/surfactant ≥ 5 (Figure 7).

This growth mechanism gives hybrid micellar objects that can be described as in Figure 9. They evolve from pure micelles ([TEOS] = 0) (top) to one where small silica oligomers (undetected by DLS and SAXS) polymerize in the palisade layer for Si/surfactant = 4 (middle). Several hypotheses explain why silica polymerizes at pH 2−4, in the PEO shell, but not in bulk water. Terminal OH groups of the PEO chains are more nucleophilic than water, and interactions between bound water molecules acting as general bases and EO groups make them good nucleophiles.[26−29] In addition, the relative local concentration of silica oligomers confined in the PEO shells is considerably higher than that in bulk water, and the local arrangement of molecules in this shell reduces the entropic loss in polymerization and therefore assists reaction. However, as for F^--catalyzed pure silica gelation in these conditions and the insignificant changes in the forms of SAXS patterns (Figure 7), silica densities must be very low. As Si/surfactant increases above 4, these low-reticulated oligomers extend out of the palisade layer, but we may think that the polymerization reaction still occurs in it, giving the linear diameter increase detected by DLS (Figure 6). The high stability of these hybrid objects makes them good candidates for specific studies dealing with interactions between silica and nonionic micelles, such as the structural modifications during the condensation step. Moreover, they also are promising building units in syntheses of new materials.

In the synthesis of mesoporous MSU-X silica according to our two-step pathway, the subsequent step is condensation of these hybrid silica micelles catalyzed either by dilute F^- or by increasing the pH.[16] Fluoride ions assist better assembly of these "bricks", and the subsequent restructuring generates a 3D wormhole porous structure. The in situ study of the first moments of this reaction shows that the association of these hybrid units gives within 10 min well-structured seeds of the future material.

V. Appendix: Water/Silica Molar Ratio in the Outer Shell

The silica on water ratio in the outer silica shell around micelles was calculated as outlined below.

V.1. Calculation of the Amount of Micelles in 100 cm³. Tergitol 15-S-12 being a $C_{15}(EO)_{12}$ molecule (MW = 738), in 100 cm^3 of a 0.02 M solution of T15S12, that is, in 1.476 g of T15S12, one may assume that there are 0.422 g of oil (the pentadecane tail in the hydrophobic core). Assuming that the alkyl tail in the hydrophobic core exhibits a structure to that of a liquid (G. Porte, private communication), one may assign the density of pentadecane (0.77, *Handbook of Chemistry*) to this core. Thus, the total volume of the alkyl part in 100 cm^3 of the micellar solution is

$$\frac{0.422}{0.77} = 0.548 \text{ cm}^3 \qquad (1)$$

Since the hydrophobic core diameter can be assumed to be equal to about two lengths of elongated pentadecane molecules, that is, 3 nm, the volume of the hydrophobic core is

$$\frac{4\pi}{3}(1.5\ 10^{-7}\text{ cm})^3 = 1.414 \times 10^{-20}\text{ cm}^3 \qquad (2)$$

Thus, the number of micelles in 100 cm^3 can be easily deduced:

$$\frac{\text{total vol. of pentadecane}}{\text{vol. of one core}} = \frac{0.548}{1.414 \times 10^{-20}} = 3.876 \times 10^{19}$$

The previous result allows us to calculate the expected number of surfactant molecules per micelle: in 100 cm^3 $[(2 \times 10^{-3})(6.023 \times 10^{23}) = 1.205 \times 10^{21}$ molecules], one

(26) El Seoud, O. A. *Adv. Colloid Interface Sci.* **1989**, *30*, 1.
(27) Bunton, C. A.; Forovodian, H. J.; Gillitt, N. D.; Whiddon, C. *Can. J. Chem.* **1998**, *76*, 946.
(28) Romsted, L. S.; Yao, J. *Langmuir* **1996**, *12*, 2425.
(29) Romsted, L. S.; Yao, J. *Langmuir* **1999**, *15*, 326.

finds that there are $(1.205 \times 10^{21})/(3.876 \times 10^{19}) = 31$ molecules/micelle.

V.2. Calculation of the Total Volume of the Silica Network around the Micelles in 100 cm^3. The volume of the hybrid objects obtained for a Si/TA ratio of 20 (diameter of 10.5 nm) is Therefore, the volume

$$\frac{4\pi}{3}(5.2 \times 10^{-7}\ \text{cm})^3 = 58.9 \times 10^{-20}\ \text{cm}^3 \qquad (3)$$

occupied by the silica network for one micelle is 58.9×10^{-20} (volume of the hybrid micelle) $- 1.414 \times 10^{-20}$ (volume of the hydrophobic core) $= 57.5 \times 10^{-20}$ cm^3, to be multiplied by the number of micelles in 100 cm^3: $(57.5 \times 10^{-20})(3.876 \times 10^{19}) = 22.28$ cm^3.

V.3. Calculation of the Water/Silica Molar Ratio in the Silica Network around the Micelles. In 22.28 cm^3, the total number of water moles is close to 1.24.

For the reaction, one uses a Si/TA ratio of 20, that is, a Si concentration of 0.4 mol·L^{-1}. In 100 cm^3, all the 0.04 mol is assumed to be in the silica network. Hence, the water/silica molar ratio is $1.24/0.04 = 31$.

Acknowledgment. E.P. and C.B. thank J. Appell and M. Henry for fruitful discussions regarding the assembly model herein described.

CM011031B